

Deuteration of Heptamethine Cyanine Dyes Leads to Enhanced Emission Efficacy

Hana Janeková,¹ Hannah C. Friedman,² Marina Russo,¹ Mergime Zyberaj,¹ Tasnim Ahmed,² Ash Sueh Hua,² Anthony V. Sica,² Justin R. Caram,^{2,*} Peter Štacko^{1,*}

¹ Department of Chemistry, University of Zurich, Winterthurerstrasse 190, 8057 Zurich, Switzerland

² Department of Chemistry and Biochemistry, University of California, Los Angeles, 607 Charles E. Young Drive, Los Angeles, CA 90095-1569, USA

Abstract

Short-wave infrared region (SWIR; 900–2000 nm) enables *in vivo* bioimaging with unrivaled spatial and temporal resolution, but its full potential is locked behind the lack of highly emissive organic fluorophores. Their design remains a grand challenge and understanding the structure-property relationship is the key to their rational design. Here we investigate the effects of deuteration on the photophysical properties of a series of heptamethine (Cy7) dyes bearing different terminal heterocycles, the absorption of which spans the near-infrared (NIR) and SWIR regions. Using cheap deuterium sources, we demonstrate that deuteration is a strategy applicable across the Cy7 family that leads to enhanced quantum yields of fluorescence, longer-lived singlet excited states and suppressed rates of non-radiative deactivation processes. Jointly with exclusion of the central cyclohexenyl ring, the approach furnishes the brightest SWIR-emitting Cy7 fluorophore disclosed to this date.

Introduction

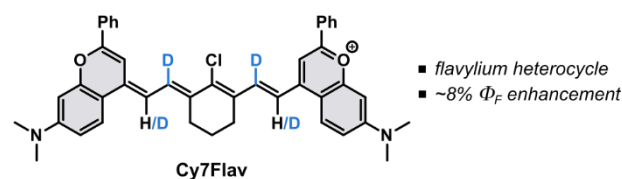
The move towards short-wave infrared (SWIR; 900–2000 nm) region has recently emerged as a complementary approach to enhance bioimaging techniques with unrivaled spatiotemporal resolution.¹ The feasibility of SWIR imaging was demonstrated *in vivo* using carbon nanotubes,² quantum dots,³ rare-earth nanomaterials⁴ and small molecules.⁵ The full potential of SWIR imaging in terms of deep penetration, high spatial resolution, multicolor imaging and fast acquisition rates was showcased using quantum dots.⁶ Their high emission quantum yield enabled quantification of heartbeat and breathing rates in awake animals and construction of a brain vasculature map. SWIR imaging was recently employed to realize excitation multiplexing in awake animals with video-rate *in vivo* imaging.^{7,8}

However, the full potential of bioimaging in SWIR region is restricted by critically underperforming organic small-molecules-based fluorescent probes with fluorescence quantum yields (Φ_F) generally below 1%. The existing probes are usually based on donor–acceptor–donor motif or, more commonly, cyanine scaffold (Cy7).^{5,9–14} We and Schnermann have shown that the low Φ_F of Cy7 cyanines are linked to fast non-radiative deactivation processes in the singlet excited state instead of *E–Z* photoisomerization.^{15,16} The rate of these processes increases exponentially with the decreasing HOMO–LUMO energy gap (i.e. red-shifted absorption maximum), also known as the “energy gap law”.¹⁷ As a result, the design of bright and efficient organic SWIR fluorophores remains a grand challenge. Besides SWIR applications, extending the lifetimes is crucial also in the context of other applications that rely on chemistry occurring from the excited state.^{18–22}

Some of us recently conceptualized the deuteration of cyanine scaffold as a potentially productive avenue to highly emissive SWIR fluorophores (Figure 1) *via* suppression of non-radiative deactivation rates, owed to stiffer and less energetic C–D stretching vibrations ($\tilde{\nu}$ ~2200 cm⁻¹) compared to those of C–H ($\tilde{\nu}$

~3100 cm⁻¹).²³ Recently, deuteration of *N*-methyl substituents in rhodamines resulted in a significant increase of their Φ_F .²⁴ Besides affecting emission properties, deuteration has been shown to increase the thermal stability of indocyanine green (ICG) and extend its shelf life harnessing the kinetic isotope effect.²⁵ Herein, we investigate the deuteration along the entire central chain in a series of near-infrared- and SWIR-emitting Cy7 dyes bearing different terminal heterocycles as a general strategy to enhance their emissive properties.

PREVIOUS WORK



THIS WORK

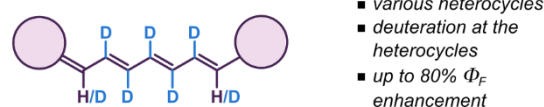
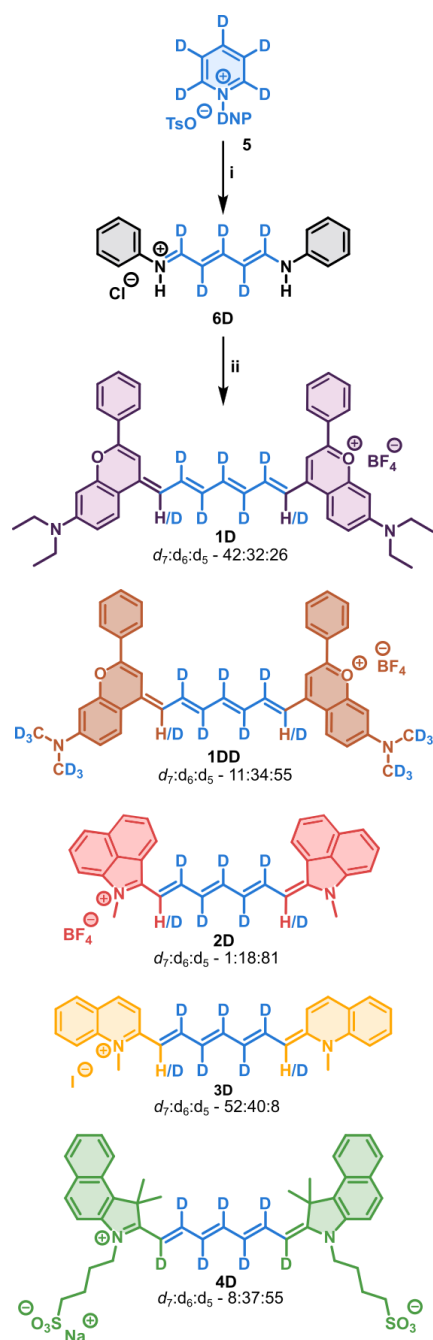


Figure 1. Comparison of the state-of-the-art with this work.

Results and Discussion

Cyanines **1–4D** were synthesized from pyridine-*d*₅ as a cheap and readily available source of deuterium atoms (Scheme 1). Pyridine-*d*₅ was transformed to the corresponding Zincke salt **5**,²⁶ and subsequently ring-opened using aniline in D₂O/CD₃OD to provide intermediate **6D** in a good overall yield. The intermediate **6D** was activated by *in-situ* acetylation using Ac₂O and subsequently condensed with the corresponding terminal heterocycles **9–13** to provide deuterated Cy7 **1–4D**. The final compounds were obtained as mixtures of *d*₇:*d*₆:*d*₅ in variable



Scheme 1. Synthesis of cyanines. **1–4D**: i) 1. PhNH₂, CD₃OD/D₂O, r.t.; 2. HCl (32%), *i*PrOH; 57%. ii) 1. CH₃CN, DIPEA, Ac₂O, rt; 2. heterocycle **10**, CD₃OD/CD₃CN, r.t.; 54% for **1D**. **2D**: Ac₂O, **13**, CD₃OD, AcONa, r.t., 52%. For **3D** and **4D** 1. CH₃CN, DIPEA, Ac₂O, r.t., 10 min., 2. **11**, CD₃OD/CD₃CN, r.t., 18 h, yield 70% (**3D**); 47% (**4D**). **1H–3H** were prepared in analogous fashion using non-deuterated solvents.

ratios determined from isotope pattern of HRMS. In case of **1H–D**, intensive degassing was necessary to prevent oxidation of the flavylium heterocycle **10** as observed previously by Sletten and co-workers.²⁷ The degree of deuteration at C1' and C7' positions is related to the ability of the heterocycle to undergo deuterium exchange at the activated methyl under the reaction conditions. Premixing heterocycle **10** in *d*₄-CD₃OD led to no discernable deuterium enrichment at the methyl after 1 hour (<5%), presumably due to low acidity of the hydrogens (Figure S57). Addition of Et₃N to promote the exchange by quantitative transformation of **10** to its analogue containing an exocyclic

double bond provided no additional deuterium incorporation on this timescale. Analogously, premixing the heterocycle **13** in CD₃OD with AcONa did not improve the ratio of deuterium incorporated in the cyanine **2D**. The deuteria contained in the heterocycle **9** required for **1DD** were introduced by methylation of the starting 3-aminophenol with CD₃I (see Supporting Information). The protonated derivatives **1–3H** were prepared in analogous fashion starting from the commercial **6H**.

Photophysical and photochemical properties of the synthesized fluorophores are summarized in Table 1. The measurements were performed in dichloromethane (DCM) to decouple the investigations from aggregation phenomena, and to facilitate straightforward comparison with the values reported in the literature. Deuteration of the heptamethine chain showed negligible effect on the absorption properties of **1–4D** and led only to a minor shift of their absorption maxima (Figure 2A–B). The derivatives **1H**, **1D**, **1DD** and **2H–D** possess absorption maxima at ~990 nm and emission maxima above ~1020 nm, consistent with analogous derivatives.¹² Consistent with the literature,^{16,25} derivatives **3D** and **4D** display more blue shifted absorption maxima at 832 and 782 nm, respectively, and ~30 and ~50 nm Stokes shifts, respectively. All the derivatives show large molar absorption coefficients that are typical for Cy7 dyes.^{7,16,28}

The emerging importance of cyanines as SWIR fluorophores motivated us to investigate the effect of deuteration on their quantum yields of fluorescence (Φ_F). In general, the deuterated analogues demonstrated a clear enhancement of Φ_F ($\chi = 100 \times (\Phi_D/\Phi_H - 1)$), whereas the protonated parent compounds showed Φ_F values consistent with the literature (Figure 2C).^{7,16} Specifically, cyanines **1D**, **1DD**, **2D** and **4D** display χ of 17%, 80%, 9%, and 12%, respectively, whereas the quinolinium derivative **3D** exhibits a relative decrease of 17%. We attribute the origin of this outlier to its very weak emission ($\Phi_F < 0.06\%$) that is at the very limit of the InGaAs detector, introducing a large experimental error. The observed χ for **4H–D** was also comparable to the results of Smith and co-workers obtained in DMSO.²⁵ **1DD** was prepared to evaluate if χ increases with the degree of deuteration. Indeed, **1DD** incorporating higher deuterium content experienced significantly higher χ compared to that of **1D**. With the total brightness of 7080 M⁻¹ cm⁻¹, **1DD** is 4.8-fold brighter than the previously best performing flavylium-based Cy7, and substantially brighter than the structurally related chromenylum analogue (~65%).⁸

Excluding **1DD**, no clear correlation of χ with the HOMO-LUMO energy gap (i.e. the absorption maxima) was observed in our series (Figure 3C) as would be expected from the energy gap law. Intrigued by this, we decided to consider other potential deactivation pathways since the efficacy of the fluorophore is limited by the worst deactivation pathway. Φ_F of **1D** is not improved in more viscous DMSO ($\eta=2.0$ cP) compared to DCM ($\eta=0.5$ cP), suggesting that rotation of the phenyl substituent at the flavylium core is also not significantly involved in the deactivation (Figure S52). The excellent work of Sletten also provides important insights in this regard.⁸ They showed that, unlike in other chromophores, introduction of julolidine to restrict the motion around the C–N bond does not improve Φ_F , suggesting twisted intramolecular charge transfer (TICT) is not a major deactivation pathway. At the same time, introduction of a *tert*-Bu substituent

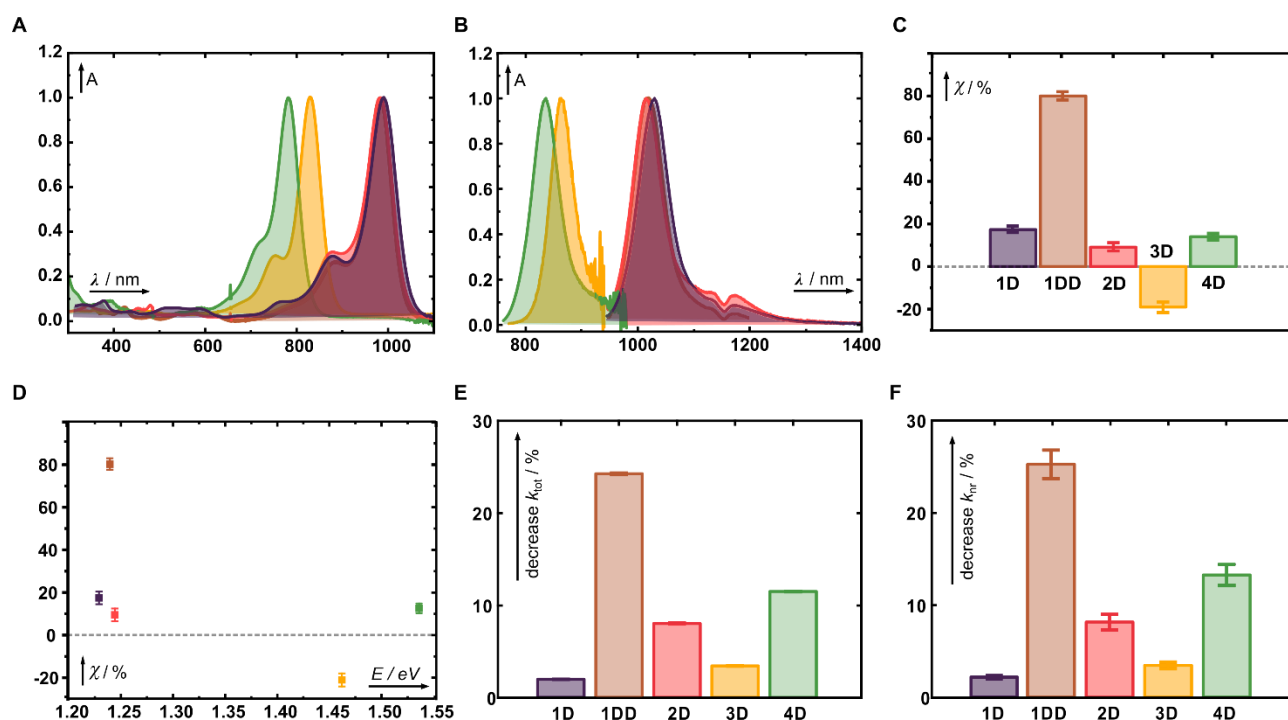


Figure 2. a) UV-Vis absorption spectra of **1D–4D** in DCM. b) Emission spectra of **1D–4D** in DCM. c) Enhancement (χ) of Φ_F in **1D–4D** induced by deuteration of the Cy7 scaffold. d) Enhancement (χ) of Φ_F in **1D–4D** as a function of the HOMO-LUMO gap. e) Percent difference for k_{tot} . f) Percent difference for k_{nr} .

Table 1. Photophysical properties of the studied Cy7 fluorophores.

	λ_{abs}/nm^a	λ_{em}/nm^a	$\epsilon^{a,b}$	$d^c/\%$	$\Phi_F \times 10^2^{a,d}$	$\chi^e/\%$	$\epsilon \Phi_F$
1H	992	1029	280 800	—	1.33±0.08	—	3730
1D	990	1022	268 700	14	1.56±0.09	17±0.9	4190
1DD	982	1015	296 300	47	2.39±0.02	80±0.8	7080
2H	987	1014	236 900	—	0.33±0.026	—	780
2D	986	1011	219 900	21	0.36±0.025	9.9±0.9	790
3H	832	860	224 300	—	0.06±0.004	—	130
3D	832	860	237 900	26	0.05±0.004	-17±1.0	120
4H	784 ^f	830	226 000 ^f	—	11.5±0.6	—	26 000
4D	782 ^f	834	169 700 ^f	12	13.1±0.9	14±0.9	22 230

^aDetermined in DCM with 0.4% of DMSO. ^bThe molar absorption coefficient, $\epsilon_{max}/mol^{-1} dm^3 cm^{-1}$. ^cOverall degree of the deuteration. ^dQuantum yield of fluorescence relative to the reference. Average and standard deviations of the mean are given. ^eEnhancement of the quantum yield of fluorescence by deuteration defined as $\chi = 100 \times (\Phi_D/\Phi_H - 1)$. ^fDetermined in MeOH with 0.4% DMSO due to its aggregation in DCM.

in the 2-position of the heterocycles improved Φ_F by 2.8-fold. Therefore, we conclude that different C–H vibrations, e.g. located on the terminal aromatic rings, are likely significantly more efficient at dissipating the energy of the excited state in different Cy7 scaffolds. This view is consistent with the previous work of Hirata on perdeuterated aromatic amines.²⁹ In this context, deuteration of the heterocycles in combination with their modification, especially in the 2-position, may be a path forward to bright SWIR fluorophores.

Notably, we also observed a large, 3-fold increase of Φ_F in **1H** compared to its analogue containing a cyclohexenyl ring embedded in the central chain.^{8,23} This is contrary to the popular notion in the literature that the ring increases Φ_F of Cy7 dyes

through rigidification and suppression of the potential *E–Z* photoisomerization. While this structural feature provides benefits from the synthetic point of view, we have recently shown that it provides no improvements of photophysical properties.¹⁶ Little improvement of Φ_F via complete rigidification of the Cy7 scaffold observed by Schnermann and co-workers further corroborates this notion.¹⁵ Nevertheless, the explicit negative influence of the ring on Φ_F was unexpected. We speculated whether the large Φ_F increase is due to elimination of the deactivation pathways conferred by the additional C–H bonds in the ring, decreased Φ_{ISC} due to eliminating potential heavy atom effects of Cl atom, or solely because of the absence of the mildly electron accepting substitution in the C4' position (i.e. ~40 nm

Table 2: Time resolved fluorescence lifetimes and rates of Cy7 fluorophores.^a

	τ / ps	$k_{\text{tot}}/10^9 \text{ s}^{-1}$	h^b / %	$k_{\text{r}}/10^6 \text{ s}^{-1}$	h^b / %	$k_{\text{nr}}/10^9 \text{ s}^{-1}$	h^b / %
1H	118.9±0.4	8.41±0.03		112±7	—	8.29±0.05	—
1D	121.3±0.4	8.24±0.03	1.95±0.01	129±7	-15±1	8.11±0.05	2.2±0.2
1DD	158.7±1.0	6.3±0.04	24.2±1	142±1	-27±2	6.23±0.06	25±2
2H	48.5±0.2	20.6±0.1		68±5	—	20.5±2	—
2D	52.9±0.2	18.9±0.08	8.00±0.05	68±4	-0.37±0.04	18.9±1	8.0±0.8
3H	83.3±0.5	12.0±0.07		7.2±0.5	—	12.0±0.8	—
3D	86.2±0.4	11.6±0.06	3.41±0.03	5.8±0.5	19±2	11.5±0.9	3.4±0.8
4H	490.2±2.4	2.04±0.01		234±10	—	1.80±0.1	—
4D	555.5±3.0	1.80±0.01	11.46±0.04	236±15	-0.85±0.07	1.56±0.09	13±1

^aDetermined in pure DCM ^bPercent of the rate of decrease by deuteration defined as $h = 100 \times (1 - k_{\text{D}} / k_{\text{H}})$, $k_{\text{r}} = \Phi_{\text{F}} \times k_{\text{tot}}$, $k_{\text{nr}} = k_{\text{tot}} - k_{\text{r}}$

blue shift of maxima). For the latter, independent energy gap parameter as described by Caram and coworkers,²³ shows a value of 0.5 which is indicative of an increase quantum yield compared to the cyclohexyl ring analogue beyond that of the blue shift. Modification of the C4' position or deuteration of the cyclohexyl ring could elucidate the source of the improvement in the quantum yield.

To corroborate these observations, we utilized time-resolved emission spectroscopy to gain additional insight into the effect of deuteration on the excited state lifetimes and the rates of non-radiative deactivation processes. We observed a decrease in non-radiative rate upon deuteration in the entire series of Cy7 dyes, with **1DD** exhibiting improvement that is statistically significant *via* *t*-test ($p < 0.05$), which indicates that deuteration is eliminating deactivation pathways in all dyes. Additionally, all these dyes are at least 40 nm blue shifted from the parent cyclohexyl **Cy7Flav** analogue, which means that the non-radiative energy gap law for internal conversion would be less impactful to the change in quantum yield. On the other hand, **1DD** may show decrease in non-radiative rate because TICT of the amine may dominate rate in the linear dyes more because of this blue shift. When analyzing a percent decrease in rate compared to the rate for the protonated analogue, we observe smaller changes than those found in the quantum yield analysis. Using this analysis on the previously reported **Cy7Flav** derivatives,²³ we observe similar percent decrease values for non-radiative rate for the partially deuterated compounds ($4.11 \pm 0.01\%$ and $5.48 \pm 0.02\%$ for deuteration degrees of 2 and 2.12 in **Cy7Flav** scaffold, respectively). More interestingly, the rate decrease for the radiative rate is $1.11 \pm 0.06\%$ and $2.2 \pm 0.2\%$, respectively, which is much lower change than the **1D** change in the radiative rate. Though much more scanning of the synthetic space must be considered, this may be indicative of deuteration impacting the transition dipole moment in certain derivatives.

Conclusions

In conclusion, we demonstrate that deuteration is a valuable strategy applicable across the family of SWIR-absorbing Cy7 fluorophores to increase their emission efficacy and suppress the competing non-radiative deactivation pathways. We believe that the valuable lessons learned herein will guide the rational design of SWIR fluorophores and spur the investigations to identify bond vibrations which represent the greatest offenders in this context, or inspire alternative approaches to suppress these non-productive pathways, e.g. *via* perfluorination of the central polymethine chain or the appending heterocycles ($\tilde{\nu}$ of C–F $\sim 1200 \text{ cm}^{-1}$).

Acknowledgment

We gratefully acknowledge Swiss National Science Foundation (P.Š/PZ00P2_193425), the Department of Chemistry, University of Zurich (Legerlotz Stiftung, UZH Candoc), and especially the Prof. Hans E. Schmid Stiftung for funding this research project. We would like to thank Prof. Cristina Nevado, Prof. Karl Gademann and Prof. Michal Juriček (all from University of Zurich) for the generous support of our research. Justin, Hannah, Tasnim, Ash, and Anthony would like to acknowledge support from the U.S. National Science Foundation (CHE-1905242, CHE-1945572), U.S. National Institute of Biomedical Imaging and Bioengineering (1R01EB027172), and instrumentation grants U.S. National Science Foundation (CHE-1048804) and U.S. National Institute of Health (1S10OD016387).

References

- (1) Hong, G.; Antaris, A. L.; Dai, H. *Nat. Biomed. Eng.* **2017**, *1*, 1–11.
- (2) Welsher, K.; Liu, Z.; Sherlock, S. P.; Robinson, J. T.; Chen, Z.; Daranciang, D.; Dai, H. *Nat. Nanotechnol.* **2009**, *4*, 773–780.
- (3) Hong, G.; Robinson, J. T.; Zhang, Y.; Diao, S.; Antaris, A. L.; Wang, Q.; Dai, H. *Angew. Chem. Int. Ed.* **2012**, *51*, 9818–9821.
- (4) Naczynski, D. J.; Tan, M. C.; Zevon, M.; Wall, B.; Kohl, J.; Kulesa, A.; Chen, S.; Roth, C. M.; Riman, R. E.; Moghe, P. V. *Nat. Commun.* **2013**, *4*, 1–10.
- (5) Tao, Z.; Hong, G.; Shinji, C.; Chen, C.; Diao, S.; Antaris, A. L.; Zhang, B.; Zou, Y.; Dai, H. *Angew. Chem. Int. Ed.* **2013**, *52*, 13002–13006.
- (6) Bruns, O. T.; Bischof, T. S.; Harris, D. K.; Franke, D.; Shi, Y.; Riedemann, L.; Bartelt, A.; Jaworski, F. B.; Carr, J. A.; Rowlands, C. J.; et al. *Nat. Biomed. Eng.* **2017**, *1*, 1–11.
- (7) Cosco, E. D.; Spearman, A. L.; Ramakrishnan, S.; Lingg, J. G. P.; Saccomano, M.; Pengshung, M.; Arús, B. A.; Wong, K. C. Y.; Glasl, S.; Ntziachristos, V.; et al. *Nat. Chem.* **2020**, *12*, 1123–1130.
- (8) Cosco, E. D.; Arús, B. A.; Spearman, A. L.; Atallah, T. L.; Lim, I.; Leland, O. S.; Caram, J. R.; Bischof, T. S.; Bruns, O. T.; Sletten, E. M. *J. Am. Chem. Soc.* **2021**, *143*, 6836–6846.
- (9) Zhu, S.; Tian, R.; Antaris, A. L.; Chen, X.; Dai, H. *Adv. Mater.* **2019**, *31*, 1900321.
- (10) Ding, F.; Zhan, Y.; Lu, X.; Sun, Y. *Chem. Sci.* **2018**, *9*, 4370–4380.
- (11) Wang, S.; Fan, Y.; Li, D.; Sun, C.; Lei, Z.; Lu, L.; Wang, T.; Zhang, F. *Nat. Commun.* **2019**, *10*, 1–11.
- (12) Cosco, E. D.; Caram, J. R.; Bruns, O. T.; Franke, D.; Day, R. A.; Farr, E. P.; Bawendi, M. G.; Sletten, E. M. *Angew. Chem. Int. Ed.* **2017**, *56*, 13126–13129.
- (13) Li, B.; Lu, L.; Zhao, M.; Lei, Z.; Zhang, F. *Angew. Chem. Int. Ed.* **2018**, *57*, 7483–7487.
- (14) Lei, Z.; Sun, C.; Pei, P.; Wang, S.; Li, D.; Zhang, X.; Zhang, F. *Angew. Chem. Int. Ed.* **2019**, *58*, 8166–8171.
- (15) Matikonda, S. S.; Hammersley, G.; Kumari, N.; Grabenhorst, L.; Glembockyte, V.; Tinnefeld, P.; Ivanic, J.; Levitus, M.; Schnermann, M. *J. Org. Chem.* **2020**, *85*, 5907–5915.
- (16) Šťacková, L.; Muchová, E.; Russo, M.; Slaviček, P.; Šťacko, P.; Klán, P. *J. Org. Chem.* **2020**, *85*, 9776–9790.

- (17) Henry, B. R.; Siebrand, W. Wiley-VCH Verlag GmbH, 1973.
- (18) Janeková, H.; Russo, M.; Ziegler, U.; Štacko, P. *Angew. Chem. Int. Ed.* **2022**, e202204391.
- (19) Alachouzos, G.; Schulte, A. M.; Mondal, A.; Szymanski, W.; Feringa, B. L. *Angew. Chem. Int. Ed.* **2022**, e202201308.
- (20) Štacková, L.; Russo, M.; Muchová, L.; Orel, V.; Vitek, L.; Štacko, P.; Klán, P. *Chem. Eur. J.* **2020**, *26*, 13184–13190.
- (21) Janeková, H.; Russo, M.; Štacko, P. *Chimia* **2022**, *76*, 763.
- (22) Tovtik, R.; Muchová, E.; Štacková, L.; Slaviček, P.; Klán, P. *J. Org. Chem.* **2023**, *88*, 6728.
- (23) Friedman, H. C.; Cosco, E. D.; Atallah, T. L.; Jia, S.; Sletten, E. M.; Caram, J. R. *Chem* **2021**, *7*, 3359–3376.
- (24) Roßmann, K.; Akkaya, K. C.; Poc, P.; Charbonnier, C.; Eichhorst, J.; Gonschior, H.; Valavalkar, A.; Wendler, N.; Cordes, T.; Dietzek-Ivanšić, B.; et al. *Chem. Sci.* **2022**, *13*, 8605–8617.
- (25) Li, D. H.; Smith, B. D. *Chem. – A Eur. J.* **2021**, *27*, 14535–14542.
- (26) Štacková, L.; Štacko, P.; Klán, P. *J. Am. Chem. Soc.* **2019**, *141*, 7155–7162.
- (27) VanAllan, J. A.; Reynolds, G. A. *Tetrahedron Lett.* **1969**, *10*, 2047–2048.
- (28) Bricks, J. L.; Kachkovskii, A. D.; Slominskii, Y. L.; Gerasov, A. O.; Popov, S. V. *Dye. Pigment.* **2015**, *121*, 238–255.
- (29) Hirata, S.; Totani, K.; Watanabe, T.; Kaji, H.; Vacha, M. *Chem. Phys. Lett.* **2014**, *591*, 119–125.